# Gage Control of Film and Sheet-Forming Processes

**James B. Rawlings and I-Lung Chien**
New Technology Team, Process Measurement and Control Technology Center,
E.I. du Pont de Nemours & Company, Inc., Wilmington, DE 19880

*A new methodology for gage control of sheet and film processes is presented. A linear process model is developed that is capable of describing many of the interesting features of the process, including a noisy and moving gage sensor, significant process noise, strong coupling between the gage in different lanes, constraints on the actuators, and significant time delay between the actuators and the sensor. An automatic control of this process given this model form is designed. Novel features of the controller are that it can contend with information from a moving sensor and handle hard constraints on the actuators. Control performance and robustness to noise are demonstrated favorably via simulations.*

## Introduction

This article provides an overview of the problem and examines a proposed technology for improving gage control of sheet and film processes. The sheet- and film-forming process was chosen for study because of its economic importance. The processes used to manufacture many different types of polymer films and paper sheets share the same generic features and provide significant leverage for any improvement in gage variation that can be achieved. This article is a condensed version of a more comprehensive report prepared for DuPont by Rawlings and Chien (1993).

### *Process characteristics*

Figure 1 depicts the layout of a generic film-forming process. As in any sheet- or film-forming process, there is an area at which the sheet or film is extruded through some flow-controlling actuators and then pinned to roller conveyers. The film is then conveyed along the rollers through a process that involves stretching, heating, drying, shrinking, setting, and possibly coating. At some point a scanning sensor measures some properties of the film before it is rolled up on a drum as the final product. There may be multiple sensors at different locations in the process, and they may measure different properties of the film.

The following terms are defined. The *machine direction* is the direction in which the film is conveyed. The *cross direction* is the direction of the film's width. The thickness of the film is then measured in the direction perpendicular to both cross and machine directions. The film *gage* is another name for thickness. A *lane* refers to a particular cross-direction location. The lanes are normally numbered sequentially from one edge of the film. The *sample time* refers to some characteristic time of the process, normally the time interval at which the sensor provides its information. The sample time is expected to be the shortest time interval of interest, so that all other times can be described in terms of multiples of the sample time. The *time delay* is the number of sample times

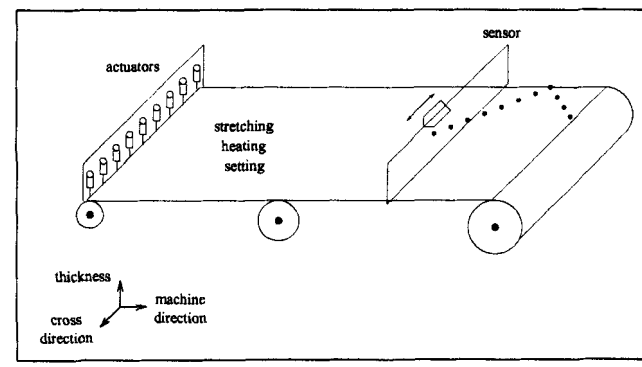


**Figure 1. Film or sheet-forming process.**

Present addresses of: J. B. Rawlings, Department of Chemical Engineering, University of Wisconsin, Madison, WI 53706; I-L. Chien, Department of Chemical Engineering, Chang Gung College of Medicine and Technology, Kwei-Shang, Taoyuan, Taiwan, R.O.C.

between when the film passes through the actuator and arrives at the sensor's machine direction location.

The sensor of main interest in this report is the *gage sensor*. The gage sensor normally consists of a radiation-emitting source and a detector. The thickness of the film is sensed by the attenuation of the radiation signal by the film. This measurement is also inherently noisy, even if the film gage is constant, and requires noise filtering. The sensor is normally mounted on a track so that it can move back and forth in the cross direction to sense the film gage in all lanes. Because the film is also moving in the machine direction, this generates a triangular-shaped pattern on the film for the points at which the film gage was actually sensed. As shown in Figure 1, the gage is only measured in a very small portion of the film. This immediately leads to one of the most discussed issues in the literature: How does one determine the gage of the film given this noisy measurement of only a small portion of the film? This issue is discussed in the following section.

The *actuator* refers to the mechanism that is manipulated by the process controller or operator to affect the gage of the film. For paper products, the actuator is often the slice lip opening. For polymer films, the actuators are often the die bolts that are exerting force on the die lip through which the polymer is extruded. For good control it may be important to have a feedback signal of true actuator movement, since the actuators may fail and the controller needs to know if the actuator is actually responding to commands. This point is discussed further in the section titled "Constrained regulation." Another valve upstream of the process is often used to manipulate the total flowrate of material into the die or headbox. This manipulated variable is typically used to reject disturbances that affect all lanes simultaneously. We do not discuss these actuators here, but it is straightforward to include them in the regulator under discussion once they are modeled.

The simplest mathematical model that can describe many of the known process characteristics is constructed in the following section. There is an extensive discussion of the sensor and process noise and how this noise can be modeled. The third section then discusses the control problem. The first issue is how best to estimate the thickness of the entire film given the sensor's noisy measurement of only a small portion of the film. The next issue is how to construct a regulator that uses this estimate of the film gage to determine the best control action to take with the actuators. It is shown that the regulator must take into account the actuator constraints in order to provide good control. Closed-loop stability of the combined estimator/regulator is discussed as well as closed-loop performance for disturbance rejection and setpoint tracking. The tuning of the controller to trade-off the competing objectives of fast dynamic response vs. low sensitivity to sensor noise is discussed and simulations are presented that compare favorably against other existing control methods. Finally the fourth section draws conclusions and describes the planned next steps in this research project.

As will become apparent in the discussion on state estimation, this work is strongly influenced by Bergh and MacGregor's (1987) approach of describing the moving gage sensor with a time-varying $C$ matrix and using Kalman filtering to reconstruct optimally the state of the film from this sensor's output. The important difference between this work and that of Bergh and MacGregor is in the regulator. The previous work recommended the standard linear quadratic regulator and therefore produced a linear quadratic Gaussian (LQG) controller. This work demonstrates the need to handle carefully the actuator constraints and recommends a constrained linear quadratic regulator, and therefore produces a model-predictive controller (Muske and Rawlings, 1993). Chen (1988) also discusses the use of Kalman filtering for this application.

In the handling of constraints by the regulator, Boyle (1977) was the first to recommend solving a quadratic program to handle hard actuator limits for cross-directional control of film-forming processes. The differences between this work and Boyle's are that Boyle used a steady-state rather than dynamic process model, did not account for the moving sensor or time delay between actuators and sensor, and did not include a disturbance model.

Braatz et al. (1992) have recently discussed implementation of cross-directional control for coating processes. Some differences between this approach and theirs are they approximate the process dynamics with a pure delay, do not consider the moving sensor, and use a first-order filter for noise filtering. They implement actuator constraints by scaling the unconstrained control moves rather than solving a quadratic program on line because it is thought to be simpler and adequate for their process. They successfully implemented their technique on a pilot-plant coating process at Avery.

## Process Model

The goal of modeling in this context is to provide the simplest mathematical model that can describe the essential features of the process. Due to the nature of feedback control, the model does not have to be extremely accurate for the controller to provide acceptable closed-loop performance.

### *Linear dynamics*

As depicted in Figure 1, consider the state to be the thickness of the film at each cross-direction sensor sample location at the sensor's machine-direction location. Associate with each of these cross-direction locations, or lanes, an integer index, $i$. The state is then a column vector of length $l$, the number of lanes, and $x_i$ represents the thickness of the film in lane $i$. Notice that with this definition of state, we are neglecting the distributed nature of the film in the machine direction and are only considering the cross direction. If one has a process with several sensors and actuators at different machine-direction locations, it might make sense to model the machine direction more carefully, but we do not take that approach in this article.

The simplest model to consider for this process is a linear, finite-dimensional, time-invariant dynamic model. In discrete time, this model has the form

$$x(k+1) = Ax(k) + Bu(k)$$
$$y(k) = Cx(k)$$

in which $x$ is the state vector (e.g., thickness of the film), $u$ is the manipulated variable or input vector (e.g., die bolt adjustment), and $y$ is the measurement or output vector. The lin-

ear assumption affords great simplification in the controller design. This assumption should be abandoned only if the data clearly indicate that nonlinearity is important and cannot be neglected without loss of control performance.

### *State transition matrix, A, and actuator matrix, B*

Imagine locating close to the die lip a fixed bank of sensors at each lane direction. This hypothetical sensor would then measure the thickness of the film in all lanes simultaneously.

Consider a step test applied to the $j$th actuator, $u_j(k) = 1$. In the absence of any noise or disturbances, the dynamic response of the bank of sensors is expected to look like Figure 2. Notice there is no time delay between actuator change and sensor response because the hypothetical sensor is assumed to be very close to the die lip. Provided the process is stable, the steady-state response is given by

$$x_s = (I - A)^{-1} B u_s.$$

The gain matrix, $K$, is defined to be the connection between steady-state input and state,

$$K = (I - A)^{-1} B.$$

If the dynamics are very fast and the system reaches steady state quickly, one may wish to approximate the system with instantaneous dynamics, which is equivalent to setting $A = 0$. In this case, $K = B$. If the dynamics are not assumed instantaneous, an alternative simple model form is to assume that the dynamic response of each lane is independent of the other lanes. The matrix $A$ is diagonal in this case.

Establishing values of $K$ is considered in numerous papers and reports (Wilhelm and Fjeld, 1983), for example. The essential features shared by the $K$ matrices in the various reports are that they are diagonally dominant and have a fairly narrow band of nonzero off-diagonal elements.

To illustrate these points, Figure 2 displays the response of the film to a step change in the middle actuator for a 10-lane film with 5 actuators. For this simulation,

$$A = 0.8 I_{10}, \quad B = (I - A)K$$

and

$$K = \begin{bmatrix} 1 & 0.6 & 0.2 & 0 & 0 \\ 0.8 & 0.8 & 0.4 & 0 & 0 \\ 0.6 & 1 & 0.6 & 0.2 & 0 \\ 0.4 & 0.8 & 0.8 & 0.4 & 0 \\ 0.2 & 0.6 & 1 & 0.6 & 0.2 \\ 0 & 0.4 & 0.8 & 0.8 & 0.4 \\ 0 & 0.2 & 0.6 & 1 & 0.6 \\ 0 & 0 & 0.4 & 0.8 & 0.8 \\ 0 & 0 & 0.2 & 0.6 & 1 \\ 0 & 0 & 0 & 0.4 & 0.8 \end{bmatrix}$$

The response of the film gage for a unit step in the first actuator is shown in Figure 3.

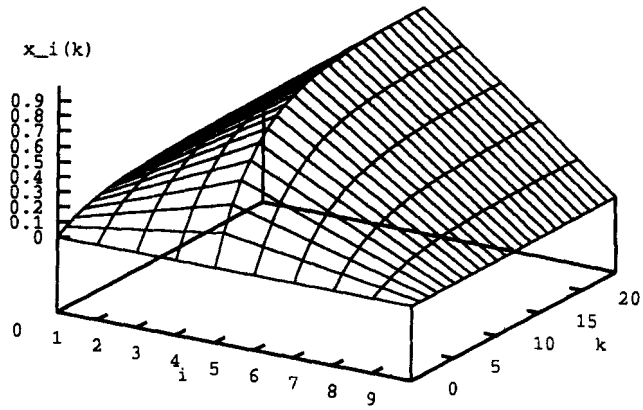


**Figure 2. Film gage for unit step in center actuator, $u_3(k) = 1$.**

### *Measurement matrix, C*

A time-invariant $C$ matrix is not adequate to describe this process because the sensor is moving. We next show how the moving sensor can be described with a time-varying $C$ matrix. This idea is due to Bergh and MacGregor (1987).

If the gage measuring device were a fixed bank of sensors at each lane location, then the $C$ matrix would be an identity matrix and the measurement vector, $y$, would be the same as the state vector, that is, the entire state would be measured. With the actual scanning sensor, however, only one lane is measured at each sample time. The $C$ matrix is therefore a time-varying row vector.

Let us consider a simple five-lane example, $l = 5$, to make this clear. Assume at time 1 that the sensor is above the first lane and $y(1) = x_1(1)$, that is, the output of the sensor at time 1 is the thickness of the film in lane 1. At the next sample time the sensor moves to lane 2 and $y(2) = x_2(2)$. Similarly, at time 3 the sensor is over lane 3, at time 4 the sensor is over lane 4, and at time 5 the sensor is over lane 5. At time 6, the sensor begins to return across the sheet and is again over lane 4, so $y(6) = x_4(6)$. This pattern of scanning is therefore represented by

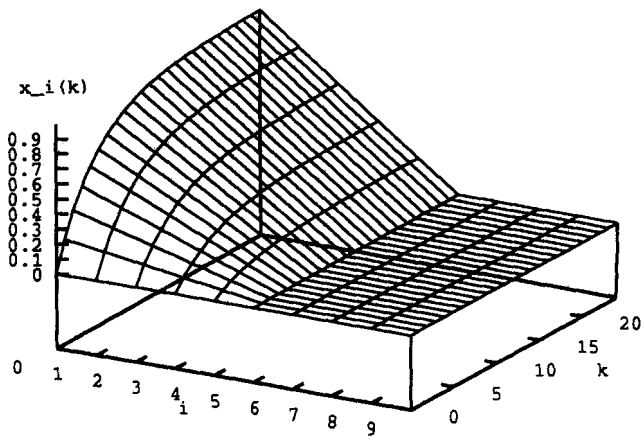


**Figure 3. Film gage for unit step in first actuator, $u_1(k) = 1$.**

$$
\begin{aligned}
y(1) &= [1 \quad 0 \quad 0 \quad 0 \quad 0]x(1)\\
y(2) &= [0 \quad 1 \quad 0 \quad 0 \quad 0]x(2)\\
y(3) &= [0 \quad 0 \quad 1 \quad 0 \quad 0]x(3)\\
y(4) &= [0 \quad 0 \quad 0 \quad 1 \quad 0]x(4)\\
y(5) &= [0 \quad 0 \quad 0 \quad 0 \quad 1]x(5)\\
y(6) &= [0 \quad 0 \quad 0 \quad 1 \quad 0]x(6)\\
y(7) &= [0 \quad 0 \quad 1 \quad 0 \quad 0]x(7)\\
y(8) &= [0 \quad 1 \quad 0 \quad 0 \quad 0]x(8).
\end{aligned}
$$

This pattern then repeats and

$$
y(9) = [1 \quad 0 \quad 0 \quad 0 \quad 0]x(9)
$$

Notice that $C(k)$ is a time-varying, periodic row vector with period $2(l-1)$. It selects the single lane location that is being sensed at each sample time. A compact way of expressing $C(k)$ is to let

$$
r = 1 + (k-1) \bmod 2(l-1).
$$

Then $C(k)$ is a row vector of zeros except for a one in the $q$th location in which

$$
\begin{aligned}
q &= r, \qquad 1 \le r \le l-1, \qquad \text{forward sensor sweep}\\
q &= 2l - r, \quad l \le r \le 2(l-1), \quad \text{return sensor sweep.}
\end{aligned}
$$

Therefore at this juncture, the proposed model form is

$$
x(k+1) = Ax(k) + Bu(k) \tag{1}
$$

$$
y(k) = C(k)x(k) \tag{2}
$$

### *Time delay*

Given the distance separating the die lip and the gage sensor and the speed of the film in the machine direction, one can calculate the time delay between the action of the actuator and response of the sensor. If the film speed is assumed approximately constant in time, the time delay is also constant and can be accounted for without difficulty. Let $d$ be the time delay in sample times. One can define an enlarged state vector, $z$, as either

$$
z(k) = \begin{bmatrix} x(k) \\ x(k+1) \\ \vdots \\ x(k+d) \end{bmatrix}
$$

or

$$
z(k) = \begin{bmatrix} x(k) \\ u(k-d) \\ \vdots \\ u(k-2) \\ u(k-1) \end{bmatrix}
$$

and a state-space model without delay for the enlarged state can be constructed. For clarity of explanation, we shall neglect the time delay in much of the subsequent discussion. The purpose of this section is to mention that inclusion of the time delay does not cause any theoretical difficulties.

### *Noise model*

The fact is that the gage sensor is noisy. This problem is compounded by the fact that the scanning gage sensor does not measure the complete state at each sample time, but only a single lane. The reconstruction of the full state from a noisy, incomplete state measurement is a key problem for all film-forming processes. Gage sensor vendor reports are full of filtering strategies to overcome this problem. We wish to revisit this issue, set up the noise problem in a fairly general setting, and then provide optimal filtering strategies for the assumed model structures. The value of this approach is that once the noise model has been assumed, the optimal filtering strategy can be determined unambiguously. If the resulting filter does not provide acceptable performance, the process model is the problem. One does not have to ask whether there could be a better filtering strategy; the filtering strategy is the unique optimal strategy given the assumed process model and noise statistics. One only has to ask why the process and noise models do not well represent the process. This important identification issue is further discussed in the conclusions section.

A simple, but reasonably flexible, model to account for noise in a system modeled by Eq. 1 is to add process noise, $w(k)$, and sensor noise, $v(k)$:

$$
x(k+1) = Ax(k) + Bu(k) + w(k) \tag{3}
$$

$$
y(k) = C(k)x(k) + v(k). \tag{4}
$$

It is convenient in filtering theory to assume that $w$ and $v$ are uncorrelated, zero mean, normally distributed, random variables, also known as white noise. Although this is probably a reasonable model for the sensor noise, it is probably not an appropriate model for the process noise. Consider the following thought experiment. Imagine the process dynamics are very fast and $A = 0$ is a reasonable assumption. Imagine also that the sensor is stationary over the $i$th lane so $y(k) = x_i(k)$. If the process starts off at the setpoint, $x(0) = 0$, and all the actuators are held at constant values, $u(k) = 0$, the model predicts that the gage sensor would measure zero mean noise with constant variance, as shown by the solid line in Figure 4. This is not necessarily a reasonable outcome. It might be more reasonable in a real film-forming process to see periods of significant drift away from the zero as shown by the dashed line in Figure 4. The noise model for the dashed line in Figure 4 is integrated white noise, also known as a random walk or Brownian motion.

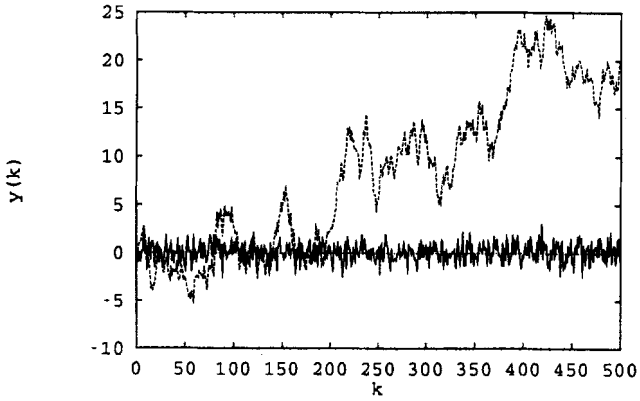


**Figure 4. White noise (—) and integrated white noise (- - - -) models.**

An important concept in control theory is the so-called internal model principle established by Francis and Wonham (1976). This principle basically states that in order for a controller to perform good disturbance rejection, the controller must have an internal model of the disturbance to be rejected. In other words, if an integrated disturbance, as shown in Figure 4, is thought to be important, one should include it in the model. This concept is also discussed by Lee et al. (1994) in the context of model predictive control. We include an integrator for the process noise by introducing a model for the state disturbance variable, $x_d$,

$$x_d(k+1) = x_d(k).$$

Again it is possible to return to the form of Eqs. 3–4 by enlarging the state vector,

$$z = \begin{bmatrix} x \\ x_d \end{bmatrix}.$$

A simulation for a 10-lane film with this noise model is presented in Figure 5. Figure 5 still does not represent a reasonable noise model for the following reason. It is highly unlikely that adjacent lanes on a sheet are affected by independent noise processes. An important source of the process noise is the processing equipment located between the actuator and sensor, pinning and stretching rolls, dryers, and so forth, as shown in Figure 1. Due to the viscoelastic nature of the polymer film, it is not likely that the process disturbances are uncorrelated between lanes. For example, an out-of-balance drum that compresses a lane in the film is likely to compress several adjacent lanes as well.

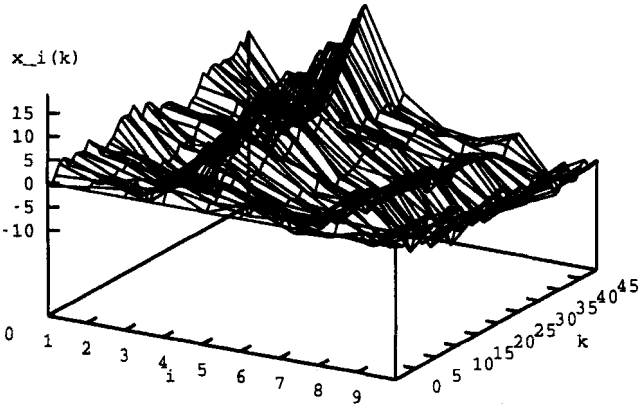


**Figure 5. Film gage for uncorrelated noise model.**

It is straightforward to include this kind of correlation in the noise process by passing the uncorrelated noise sequence, $w(k)$, through a transition matrix, $G$. The proposed noise model then takes the form

$$\begin{bmatrix} x \\ x_d \end{bmatrix}(k+1) = \begin{bmatrix} A & 0 \\ 0 & I \end{bmatrix}\begin{bmatrix} x \\ x_d \end{bmatrix}(k) + \begin{bmatrix} B \\ 0 \end{bmatrix}u(k) + \begin{bmatrix} G_x & 0 \\ 0 & G_d \end{bmatrix}w(k) \quad (5)$$

$$y(k) = C(k)[I \quad I]\begin{bmatrix} x \\ x_d \end{bmatrix}(k) + v(k). \quad (6)$$

It is expected that the $G_x$ and $G_d$ matrices will have the same diagonally dominant structure as the $B$ matrix. Let $Q$ and $R$ be the covariances of the noise sequences,

$$E\{w(j)w(k)^T\} = Q\delta(j-k)$$

$$E\{v(j)v(k)^T\} = R\delta(j-k)$$

in which $\delta(j-k)$ is the delta function defined by

$$\delta(j-k) = \begin{cases} 0 & j \neq k \\ 1 & j = k. \end{cases}$$

Figure 6 shows a 10-lane simulation using

$G_x = G_d =$

$$\begin{bmatrix} 1 & 0.6 & 0.2 & 0 & 0 & 0 & 0 & 0 & 0 & 0 \\ 0.6 & 1 & 0.6 & 0.2 & 0 & 0 & 0 & 0 & 0 & 0 \\ 0.2 & 0.6 & 1 & 0.6 & 0.2 & 0 & 0 & 0 & 0 & 0 \\ 0 & 0.2 & 0.6 & 1 & 0.6 & 0.2 & 0 & 0 & 0 & 0 \\ 0 & 0 & 0.2 & 0.6 & 1 & 0.6 & 0.2 & 0 & 0 & 0 \\ 0 & 0 & 0 & 0.2 & 0.6 & 1 & 0.6 & 0.2 & 0 & 0 \\ 0 & 0 & 0 & 0 & 0.2 & 0.6 & 1 & 0.6 & 0.2 & 0 \\ 0 & 0 & 0 & 0 & 0 & 0.2 & 0.6 & 1 & 0.6 & 0.2 \\ 0 & 0 & 0 & 0 & 0 & 0 & 0.2 & 0.6 & 1 & 0.6 \\ 0 & 0 & 0 & 0 & 0 & 0 & 0 & 0.2 & 0.6 & 1 \end{bmatrix} \quad (7)$$

and $Q = I$. The problem with the uncorrelated noise in Figure 5 is the sharp peaks in the cross direction. The correlation matrix $G$, is an identity matrix in this case. A viscoelastic fluid would not have such sharp peaks. Notice that the correlated noise shown in Figure 6 does not have such sharp variations in the cross direction.

The noise model in Eqs. 5–6 is probably the simplest model that can capture the expected features of the process behavior. Again, the identification of the appropriate $G$ matrix and covariances of the $v(k)$ and $w(k)$ noise sequences from process data are discussed in the conclusions section.

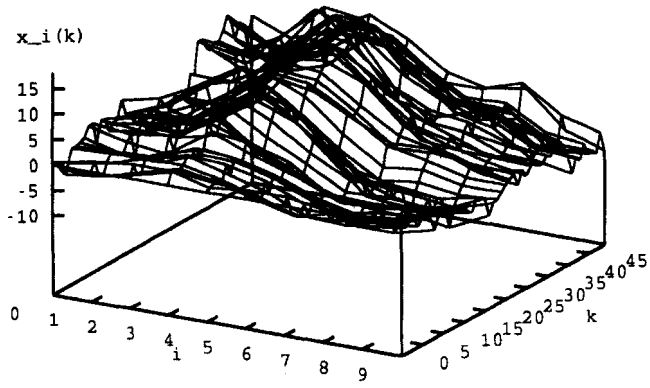


**Figure 6. Film gage for correlated noise model.**

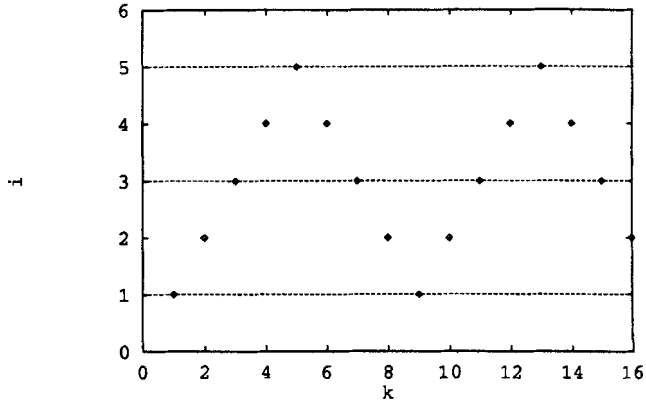


**Figure 7. Single-sample scanning pattern.**

## Control Problem

### *State estimation*

The state estimation problem can be stated as follows: Given the model, $A$, $B$, $C$, and $G$, and the noise covariances, $Q$ and $R$, and a sequence of data up to the current time $k$, $\{y(j)\}_{j=0}^{k}$, compute the optimal estimate of the state at the next sample time, $\hat{x}(k+1)$. For a linear model (time-invariant or time-varying) subject to Gaussian noise, the solution to this problem can be computed efficiently with the well-known Kalman filter. A brief review of some of the key features of the Kalman filter follows. The details and proofs are available in numerous books on stochastic control and optimal filtering (Bryson and Ho, 1975; Åström, 1970).

Consider the state-space gage model with moving sensor and Gaussian noise,

$$x(k+1) = Ax(k) + Bu(k) + Gw(k)$$
$$y(k) = C(k)x(k) + v(k).$$

The optimal estimate of $x$, $\hat{x}$ is provided by

$$\hat{x}(k+1) = A\hat{x}(k) + Bu(k) + L(k)[y(k) - C(k)\hat{x}(k)].$$

The filter gain matrix, $L(k)$, can be computed efficiently in terms of the estimate error covariance matrix, $P(k)$,

$$L(k) = AP(k)C(k)^T[C(k)P(k)C(k)^T + R]^{-1}, \quad (8)$$

in which $P(k)$ can be computed efficiently from the following Riccati iteration,

$$P(k+1) = AP(k)A^T + GQG^T$$
$$- AP(k)C(k)^T[C(k)P(k)C(k)^T + R]^{-1}C(k)P(k)A^T. \quad (9)$$

Although $L(k)$ is all that is required to compute the state estimate from the data, $P(k)$ contains important information. It is the covariance of the error in the state estimates,

$$e(k) = x(k) - \hat{x}(k).$$

In looser terms, $P(k)$ describes how much certainty one can place in the state estimate at time $k$. We subsequently show how to use $P$ to discriminate between different gage sensor designs and sampling patterns in order to choose the best ones. This analysis should be of value to the gage sensor vendors and their customers. Bergh and MacGregor (1987) point out that the time-varying, periodic $C(k)$ matrix induces time-varying, periodic $L(k)$ and $P(k)$ matrices in the optimal filter even for the asymptotic case. The computational burden of implementing the filter is still not prohibitively large, however, since the matrices can be computed off line.

We next consider a few examples to illustrate the kinds of analyses that can be done with these filters. Consider again a simple 5-lane film for illustration and let $A = 0$, $G = I$, $Q = I$, and $R = 1$. The sampling pattern is depicted in Figure 7. Using the $C(k)$ sequence corresponding to this pattern and iterating the Ricatti difference equation, Eq. 9, until the solution converges to the asymptotic, periodic values gives eight $L(k)$ column vectors and eight $10 \times 10$ $P$ matrices. The $P$ matrices are diagonal because $A$ and $G$ are diagonal in this example. The values of $P$ corresponding to $x_{d11}$ and $x_{d33}$, the edge and center values for the disturbance states, are plotted in Figure 8. These values measure the uncertainty in the state estimates. Notice that the state estimate of the edge of the film is significantly worse (large uncertainty) than the state estimate of the center of the film. Figure 8 provides a clear reason for this. Notice that the center of the film is sampled

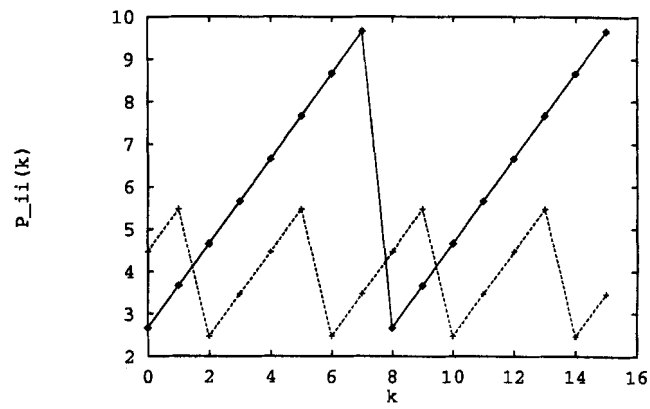


**Figure 8. State estimate error covariance for single-sample scanning, $P_{66}(k)$. Film edge (——) and $P_{88}(k)$ (film center, ---).**

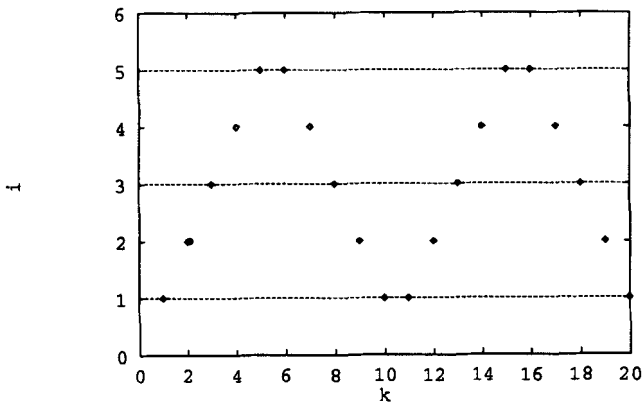


**Figure 9. Scanning pattern for double-edge scanning.**

every four sample times, twice as often as the edges of the film. The higher sampling rate provides better estimates, and Figure 8 quantifies the improvement. The intermediate lanes are sampled at uneven intervals and the covariances of the estimate errors are in between the values at the center and the edges. Notice also that because the disturbance model is integrated noise and unstable, the covariance of the estimate error in a given lane grows between samples until the sensor measures that lane again. The sensor passing over the lane gives a large reduction in the covariance of that lane at that sample time.

Next consider the same process, but a different scanning pattern. Since the gage estimates at the film edges are inferior to the rest of the lanes, one might propose to improve the overall situation by sampling the edges more often. Figure 9 depicts one such strategy. The strategy is to sample twice in succession at the edges before returning to the interior of the film. The period of this sampling strategy is 10. The calculation of the filter gains and error covariance matrices produces the center and edge error covariances plotted in Figure 10. Notice that the new strategy has not improved the estimation of the film gage. The uncertainty of the estimate of gage at the center of the film is worse since the effective sampling rate has increased from 4 to 5. The estimate of the gage at the edges of the film is also worse, however. This somewhat counterintuitive result can be explained as follows.

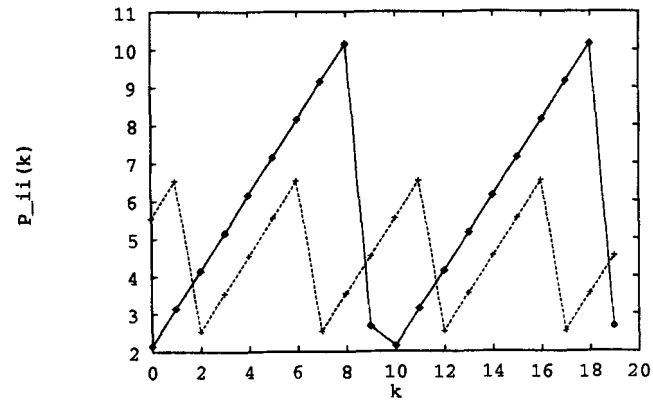


**Figure 10. State estimate error covariance for double-edge scanning, $P_{66}(k)$ (film edge, —) and $P_{88}(k)$ (film center, - - - -).**

Notice that although the edge uncertainty decreases at both sample times 9 and 10 due to the double sampling, the decrease does not make up for the increase caused by the longer period, 10 vs. 8. Although this qualitative result may be clear intuitively to a person with significant experience, the value of this analysis is that it provides a clear and quantitative method for analyzing more complicated trade-offs in sensor designs. Techniques are available for handling quantitative analysis of uncertainty given the general model, that is, nonzero $A$ and nondiagonal $G$.

As an example of how the uncertainty analysis can be used, we mention the following sensor design problem that is relevant to the next generation of gage sensors. Consider a proposed fixed bank of sensors, with the sensors spaced just as closely as the lane spacing induced by the sampling rate of a particular scanning gage sensor. The fixed bank of sensors is clearly superior to the scanning sensor since it measures all lanes simultaneously at each sample time. However, the first generation of fixed sensors is not likely to have such close spacing. The design issue is therefore how closely the fixed sensors must be placed in order to achieve a superior instrument. As soon as the technology improves to the point at which this spacing is feasible, the next generation of fixed-bank sensors can be expected to deliver improved gage control. Notice that the answer to this question depends on the process model ($A$, $G$, $Q$) as well as the sensor noise model ($R$). Certain sheet and film industries may therefore benefit from available fixed-bank sensors before other industries. These and other kinds of design issues can be simply and quantitatively assessed with this analysis.

Another method for computing the asymptotic limit of Eq. 9 is to define a time-invariant "lifted" system in which a full scan of measurements become available every $2(l-1)$ sample times. In a recent article in this journal, Tyler and Morari (1995) applied this method and evaluated the differences between fixed and scanning sensors.

As a concluding example of state estimation, we return to the ten-lane case with significant dynamics and correlated noise. Figure 11 shows the actual sheet gage for the same model as used in Figure 6. For this example, the filter gain and covariance matrices are full column vectors and matrices, respectively. Figure 12 is the optimal state estimates given the scanning gage sensor's output. Notice that the significant dynamic trends displayed by the true state are accurately reflected in the state estimate. The computational burden in

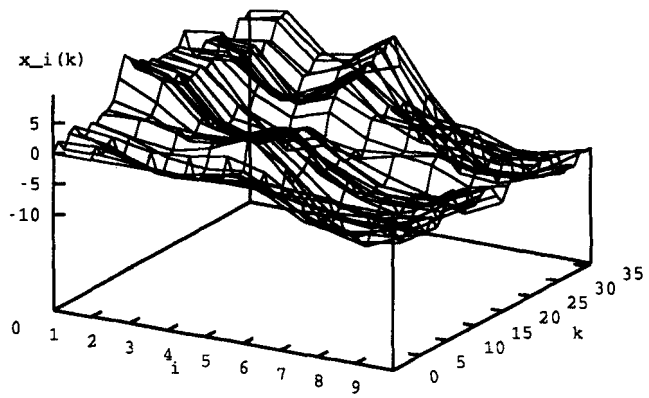


**Figure 11. True state of the film gage.**

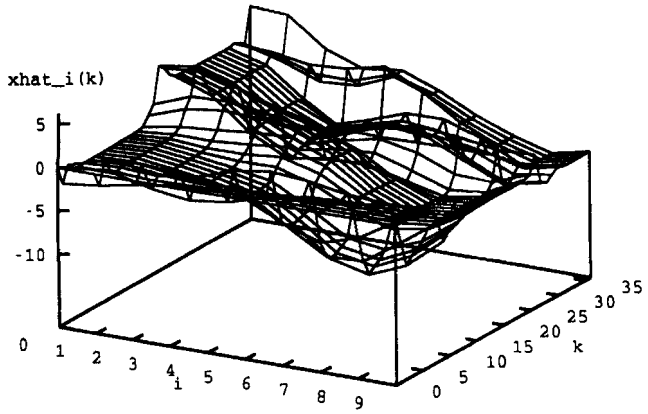


**Figure 12. Optimal state estimate of the film gage.**

implementing the optimal estimator for this ten-lane example is very small. Industrial examples that may have on the order of 100 lanes are not expected to pose large burdens on modern workstation-level computers.

*Comparison to First-Order Filtering.* In this section we assess the improvement offered by optimal state estimation vs. other simple filtering schemes that might be employed in sheet- and film-forming processes. One simple filtering approach is to assume each lane is independent and apply a first-order filter to the measurement of each lane. Thus the estimate of the thickness of lane $i$ is described by

$$\hat{x}_i(k) = (1-\alpha)\hat{x}_i(k-1) + \alpha y(k)$$

for the lane $i$ corresponding to the sensor location at time $k$. The estimates of all other lanes are left unchanged.

$$\hat{x}_j(k) = \hat{x}_j(k-1), \qquad j \neq i.$$

The tuning constant, $\alpha$, is the time constant of the filter. The filter ignores the measurement for $\alpha = 0$ and sets the estimate to the unfiltered measurement for $\alpha = 1$. The performance of this filter for $\alpha = 0.5$ is presented in Figures 13 and 14 for lanes 1 and 5. The system in the simulation is Eqs.

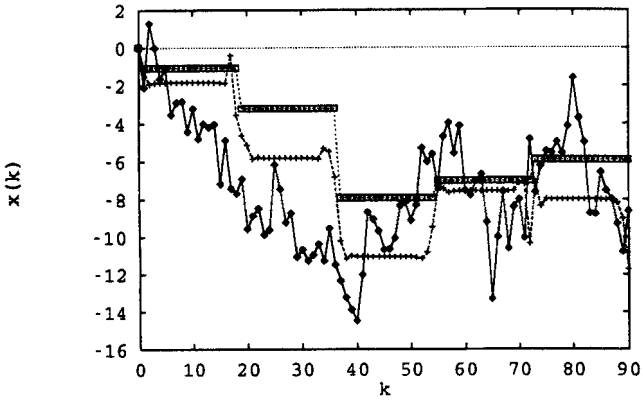


**Figure 13. Lane 1 state estimates for optimal and first-order filtering.**

True state (◇ line), optimal state estimate (+ line), and first-order filter estimate, $\alpha = 0.5$ (□ line).

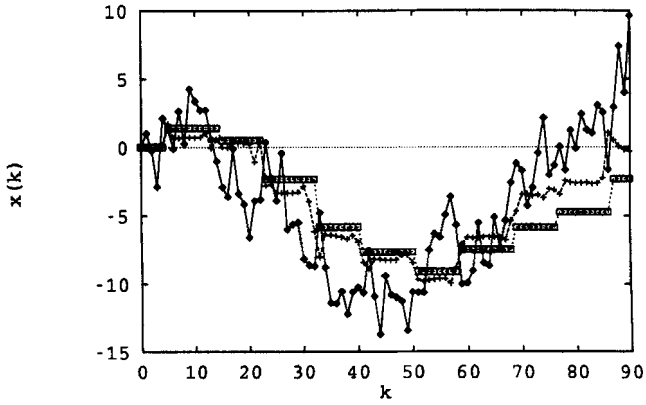


**Figure 14. Lane 5 state estimates for optimal and first-order filtering.**

True state (◇ line), optimal state estimate (+ line), and first-order filter estimate, $\alpha = 0.5$ (□ line).

5 and 6 with $A = 0$, $Q = I$, $R = 1$, and $G$ as in Eq. 7. The true state and the optimal estimates are also shown in the figures. As expected, the simple first-order filter only updates the estimate in a lane as the sensor passes over that lane. The optimal filter, which knows the correct correlation $G$ matrix, updates the state in a given lane whenever the sensor is close to that lane. This is because of the diagonal dominance of the $G$ matrix chosen for simulation.

Examination of a small number of samples in a simulation can be misleading. It is known that the optimal filter is superior to the simple first-order filter. One would like a quantitative statistical measure of how much improvement is possible. A simple quantitative measure is the mean square estimate error for a large number of samples; a more precise measure is the covariance matrix of the estimate errors for the different filter gains. The mean square error for the sheet is calculated by summing the square of the estimate errors for all the lanes at all sample times and dividing by the total number of samples. The mean square error for the sheet is summarized in Table 1 for a 10-lane sheet and 181 sample times. The mean square error for the optimal filter is 13.00. The first-order filter's mean square error for the same data is 15.86. Thus, the first-order filter's means square error is 22.0% larger than optimal. A slightly more complex filtering strategy is to use the optimal filter for uncorrelated noise, $G = I$. Using the uncorrelated filter on the same data gives a mean square error of 14.91. Thus the mean square error in these estimates is 14.7% larger than the optimal estimates, even for this diagonally dominant $G$ matrix example. In general, the larger the correlation between lanes, the larger the improvement in an optimal filter compared to filters that treat the lanes independently. Any decrease in the variance of the

**Table 1. Comparison of Optimal Filter to First-Order and Uncorrelated Filters for Ten-Lane Film and 181 Time Samples**

| | Optimal Filter | First-Order Filter $\alpha = 0.5$ | Uncorrelated Filter $G = I$ |
|---|---|---|---|
| Mean square error | 13.00 | 15.86 | 14.91 |
| increase | — | 22.0% | 14.7% |

estimate error translates into improved gage control because the controller takes actions based on better knowledge (on average) of the true state of the system. Tyler and Morari (1995) caution that if the controller must be detuned for robustness, then the improvements in gage control due to improved estimation may not be as large as expected.

### *Contrained regulation*

*Steady-State Regulation Problem.* Before proceeding to the dynamic problem, it is instructive to consider the simpler steady-state regulation problem. The steady-state relationships between $u_s$, $x_s$, $x_{ds}$, and $y_s$ are given by

$$x_s = Ku_s$$
$$y_s = x_s + x_{ds}$$

in which $K = (I - A)^{-1}B$ is the steady-state gain and $x_{ds}$ is the steady-state value of the disturbance state, which is considered known. In the actual control algorithm, this quantity is not known but estimated by the state estimator discussed in the previous section. A steady-state regulation problem can then be stated as follows: for a given $x_{ds}$ determine the steady input, $u_s$, that makes $y_s$ as small as possible. (The gage setpoint is assumed to be 0. Nonzero setpoints are handled by shifting the origin and using deviation variables.)

We next examine some solutions to this problem. The controller should be designed to not violate a number of actuator constraints. The actuators have a finite limit of travel. Adjacent actuators should not move to such opposite extremes that they create excessive local stresses in the die. We examine these constraint issues next. For illustration, we use the following gain matrix for a 5-actuator, 10-lane process,

$$K = \begin{bmatrix} 1 & 0.61 & 0.19 & 0.012 & -0.005 \\ 0.80 & 0.81 & 0.39 & 0.011 & -0.005 \\ 0.62 & 0.96 & 0.65 & 0.15 & 0.02 \\ 0.40 & 0.80 & 0.81 & 0.40 & 0.002 \\ 0.18 & 0.65 & 0.93 & 0.66 & 0.17 \\ 0.001 & 0.40 & 0.81 & 0.80 & 0.40 \\ 0.02 & 0.15 & 0.66 & 0.95 & 0.62 \\ -0.004 & 0.01 & 0.39 & 0.81 & 0.80 \\ -0.008 & 0.022 & 0.17 & 0.63 & 0.99 \\ 0.004 & -0.01 & 0.013 & 0.39 & 0.80 \end{bmatrix}.$$

Notice this $K$ matrix is similar to the one used in the section on Process Model. The steady-state regulation problem can be stated as the following optimization problem,

$$\min_{u_s} \Phi = y_s^T \Omega y_s + u_s^T \Gamma u_s, \qquad \text{(QP1)}$$

subject to

$$y_s = Ku_s + x_{ds}.$$

QP is a quadratic program. The regulator's tuning parameters are $\Omega$ and $\Gamma$. They are the positive definite weighting matrices that determine how large a penalty to place on deviations from the setpoint and amount of control action, respectively. Large values of $\Omega$ result in aggressive control action, and large values of $\Gamma$ result in conservative control action. Eq. QP1 is a simple least squares problem, and the solution is

$$u_s = -(K^T \Omega K + \Gamma)^{-1} K^T \Omega x_{ds}.$$

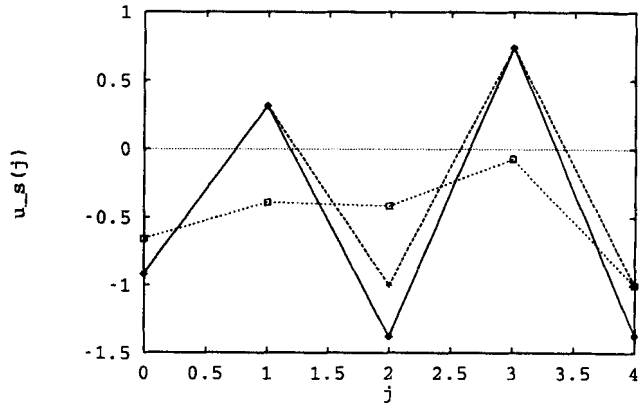


**Figure 15. Steady-state control action for $x_{ds} = 1$.**
Unconstrained least squares solution (◇ line), clipped least squares solution (+ line), and constrained solution (□ line).

Figure 15 shows the solution, $u_s$, for a state disturbance equal to 1 in each lane ($x_{ds}$ a column vector of 10 ones), $\Omega = I$, and no penalty on the input, $\Gamma = 0$. Notice that the resulting output shown in Figure 16 is close to the setpoint, but the regulator uses large control action to reject this disturbance. Assume that $-1$ represents the lower limit of travel of the actuator and is the minimum value that can be implemented. If the regulator sends out the solution to the least squares problem, then the third and fifth actuators will reach the limit of their travel and saturate. The actual input that would be delivered to the process is the *clipped* input shown by the dashed line in Figure 15. Notice that this small change in the input has led to a drastic change in the film gage, which is no longer near its setpoint. This is a characteristic feature of regulating processes that have ill-conditioned $K$ matrices. Unless prevented with careful controller design, small disturbances or

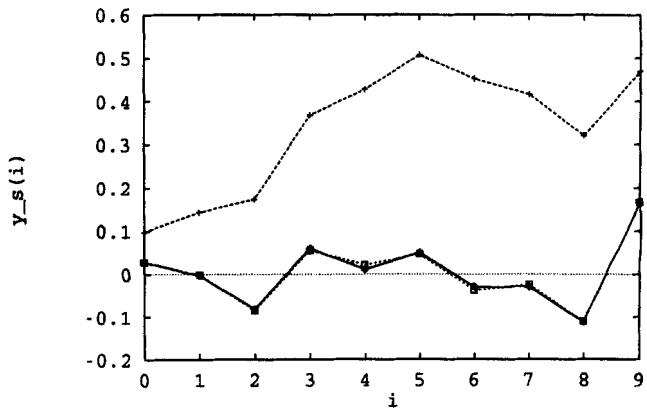


**Figure 16. Steady-state outputs corresponding to unconstrained least squares solution (◇ line), clipped least squares solution (+ line), and constrained solution (□ line).**

process model errors lead to large decreases in control performance.

One way to detune the controller to avoid this problem is to increase the input penalty. However, for ill-conditioned problems, and gage control is expected to be in this class, it is often difficult to choose the controller tuning so that the regulator does not provide extreme and undesirable control action while still tracking the setpoint closely. It is for this reason that we explore the use of constrained regulators for gage control. The first kind of constraint to consider is the restriction of the actuators reaching the limit of their travel. If the input $u$ has been normalized so that $u = -1$ is the lower limit of actuator travel and $u = 1$ is the upper limit, then the constraints are

$$\begin{bmatrix} -1 \\ -1 \\ -1 \\ -1 \\ -1 \end{bmatrix} \leq \begin{bmatrix} u_{1s} \\ u_{2s} \\ u_{3s} \\ u_{4s} \\ u_{5s} \end{bmatrix} \leq \begin{bmatrix} 1 \\ 1 \\ 1 \\ 1 \\ 1 \end{bmatrix}.$$

Convenient notation for these constraints is $u_l \leq u_s \leq u_u$ in which $u_l$ and $u_u$ are the vectors of $-1$s and 1s for the lower and upper bounds, respectively. The optimization problem for the regulator becomes

$$\min_{u_s} \Phi = y_s^T \Omega y_s + u_s^T \Gamma u_s, \qquad \text{(QP2)}$$

subject to

$$y_s = K u_s + x_{ds}$$
$$u_l \leq u_s \leq u_u.$$

The optimization problem, QP2, is a quadratic program (QP). Although its solution cannot be expressed in closed form as for the least squares problem, the solution exists, is unique, and efficient algorithms are available for calculating it (Eaton, 1993). The solution to QP2 is also shown in Figures 15 and 16. Notice that enforcing the bounds with the constrained regulator is far superior to clipping the least squares regulator. As shown in Figure 16, there is almost no loss of setpoint performance comparing the constrained regulator to the unconstrained case.

Another nice feature of constrained regulators that improves their robustness is their ability to handle actuator failures. Actuators may fail in operation for a number of causes. If the failure is detected, it is a simple matter to change the bounds in QP2 to remove the failed actuator from the set of available control actions. Consider, for example, that the center actuator has temporarily failed in the $u_{3s} = 0$ position. One can then simply change the third input bound to be $0 \leq u_{3s} \leq 0$, and the regulator will attempt to use the remaining four actuators in an optimal fashion. Figures 17 and 18 show the result of the constrained regulator compared to the simple least squares regulator, which also has the third actuator frozen in place, but is not aware of that fact and is unable to make the appropriate compensation. Notice that even in the face of the third actuator failure, the constrained regulator

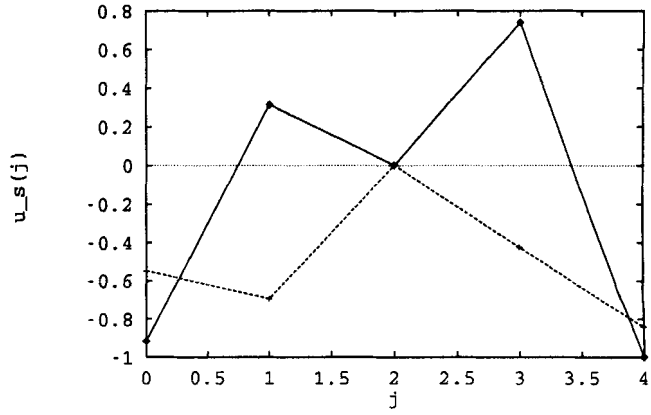


**Figure 17. Steady-state control action for $x_{ds} = 1$ and failure of the third actuator.**

Clipped least squares solution (—) and constrained solution (- - - -).

suffers little loss of performance compared to the regulator without the failure. The least squares solution that is clipped for the failed third actuator is very poor.

The second important kind of constraint is the one imposed to prevent the actuators from creating excess stress in the die. This can be expressed as a limit on the difference between adjacent actuator positions,

$$d_l \leq D u_s \leq d_u,$$

in which $d_l = -d_u$ are vectors of dimension 4 and

$$D = \begin{bmatrix} 1 & -1 & 0 & 0 & 0 \\ 0 & 1 & -1 & 0 & 0 \\ 0 & 0 & 1 & -1 & 0 \\ 0 & 0 & 0 & 1 & -1 \end{bmatrix}.$$

The final optimization problem considering both bounds on the absolute size of the inputs and differences in adjacent inputs is

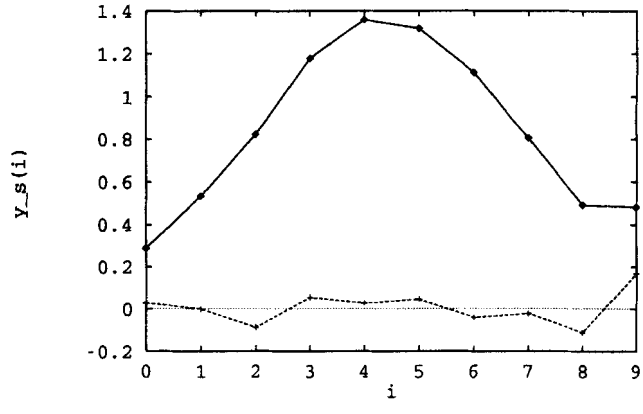


**Figure 18. Steady-state outputs for failure of the third actuator.**

Clipped least squares solution (—) and constrained solution (- - - -).

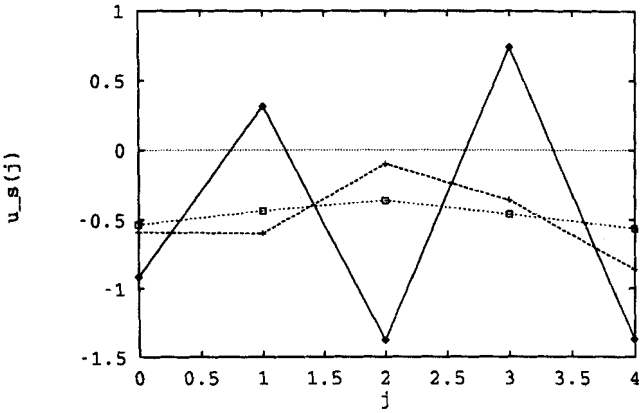


**Figure 19. Steady-state control action for $x_{ds} = 1$ and adjacent actuator difference constraints.**

Unconstrained least squares solution (◇ line), 0.5 constraint (+ line), and 0.1 constraint (□ line).

$$\min_{u_s} \Phi = y_s^T \Omega y_s + u_s^T \Gamma u_s, \qquad \text{(QP3)}$$

subject to

$$y_s = Ku_s + x_{ds}$$
$$u_l \le u_s \le u_u$$
$$d_l \le Du_s \le d_u.$$

This optimization problem, QP3, is also a QP and can be solved with available algorithms. Figures 19 and 20 show the solution using 0.5 and 0.1 as the maximum allowable differences between adjacent actuators. Notice that the controller can find a $u_s$ to satisfy the constraint set at 0.5 without much loss of performance compared to the unconstrained case. One has to accept some performance loss if the die lip cannot accept differences larger than 0.1.

In summary, constrained regulators have been shown to be significantly superior to simply clipping an unconstrained regulator. Avoiding constraint violation by penalizing the control action in the least squares regulator can be an effective alternative, but requires careful tuning. The advantage of the constrained regulator is that it does not require as much tuning and the actuator constraints are guaranteed not to be violated. Obviously appropriate use of constraints and penalties together may provide the best performance while maintaining the robustness. Boyle (1977) and Chen and Wilhelm (1986) provide further discussion of the steady-state problem with actuator constraints. Braatz et al. (1992) discuss other constraint handling methods.

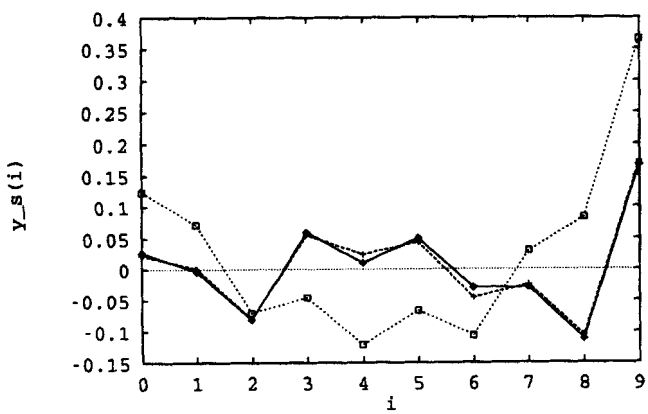


**Figure 20. Steady-state outputs for adjacent actuator difference constraints.**

Unconstrained least squares solution (◇ line), 0.5 constraint (+ line), and 0.1 constraint (□ line).

*Dynamic Regulation Problem.* The dynamic regulation problem can be addressed by using the dynamic model to predict how the current and future control actions will affect the future states over some time horizon and determining the best control action by solving an optimization problem at each time step. This approach is known as model-predictive control or receding-horizon control. Muske and Rawlings (1993) provide an overview and literature summary of model-predictive control using linear models.

Consider the following regulator optimization problem at current time $k = j$:

$$\min_{\{u(k)\}_{k=j}^{j+N-1}} \Phi = \sum_{k=j}^{\infty} x(k)^T \Omega x(k) + u(k)^T \Gamma u(k), \qquad \text{(QP4)}$$

subject to

$$\begin{aligned} x(k+1) &= Ax(k) + Bu(k), && k = j, j+1, \ldots \\ x(j) &= \hat{x}(j) \\ u_l &\le u(k) \le u_u, && k = j, j+1, \ldots \\ d_l &\le Du(k) \le d_u, && k = j, j+1, \ldots \\ u(k) &= 0 && k = j+N, j+N+1, \ldots . \end{aligned}$$

The optimal estimate of the state at time $k = j$ is provided by the state estimator. The optimal predictions of the state at times $k > j$ are given by the dynamic model with zero noise sequences, $w = 0$ and $v = 0$. The performance objective is the summed (integral) square error, and the sum is over the infinite horizon. Rawlings and Muske (1993) show that the infinite horizon objective guarantees desirable closed-loop stability properties for the regulator. Even though the horizon is infinite, the *QP* involves a finite number, $N \cdot m$, of decision variables. The control action on the remainder of the horizon is parameterized as zero. The constraints on the actuators are specified at all times $k \ge j$.

The primary tuning parameters for the regulator are $\Omega$ and $\Gamma$. The number of $u(k)$'s to be computed, $N$, is not primarily a tuning parameter. It is set large enough to provide good performance without making the real-time computational burden infeasible. The controller sends out the first move in the decision variable sequence, $u(j)$, to the process. The sensor then provides the output at the next sample time, $y(j+1)$, the estimator provides the optimal state estimate at that time, $\hat{x}(j+1)$, and problem QP4 is resolved with the new state estimate. See Muske and Rawlings (1993) for slightly more general statements of the model-predictive controller involving constraints on the time rate of change of the inputs, $u(k+1) - u(k)$, and constraints on the predicted states and outputs. The model-predictive regulator reduces to the classic linear quadratic regulator if there are no constraints and $N = \infty$.

### *Closed-loop stability*

As stated previously, the interconnection of the unconstrained optimal filter and unconstrained linear quadratic regulator is the classic LQG controller. Its properties are well-known (Åström, 1970). For the infinite-horizon case, the closed loop is stable for the nominal system for all choices of tuning parameters in the filter and regulator. However, since the steady-state gain matrix is expected to be ill-conditioned and actuator constraints are expected to be active even during normal process operation, the LQG controller is probably not the best choice for this process.

The closed-loop stability of the unconstrained optimal filter and the *constrained* linear quadratic regulator is a topic of current research. Muske (1995) shows that for feasible constraints the stabilizing state feedback control law is a Lipschitz continuous function, $u(x)$. For reconstructible systems, the estimator is exponentially stable (Campbell and Rawlings, 1994). For this case, Scokaert and Rawlings (1995) establish asymptotic stability of the interconnected estimator and regulator for all choices of tuning parameters in the filter and regulator.

We next explore the closed-loop behavior of this controller with example simulations for disturbance rejection in the presence of sensor noise.

### *Closed-loop performance*

*Disturbance Rejection.* As an illustration of the dynamic performance, consider the following example. The system is initially at steady state at the nominal setpoint in all lanes. At time zero there is a unit step change disturbance in all lanes simultaneously. Although this would have to be considered a large and rare disturbance, it is useful to watch how the combined filter and regulator deals with the disturbance. As shown in Figure 21, the true state jumps to one in each lane at $k = 0$. The sensor passes over lane 1 at $k = 1$ and measures the disturbance in lane 1 (there is no sensor noise in this first example). Although the estimator updates the state in all lanes based on this measurement, it only has enough information to update reliably lane 1. The regulator then takes the appropriate control action to eliminate the disturbance from lane 1 as shown in Figure 22. The control action

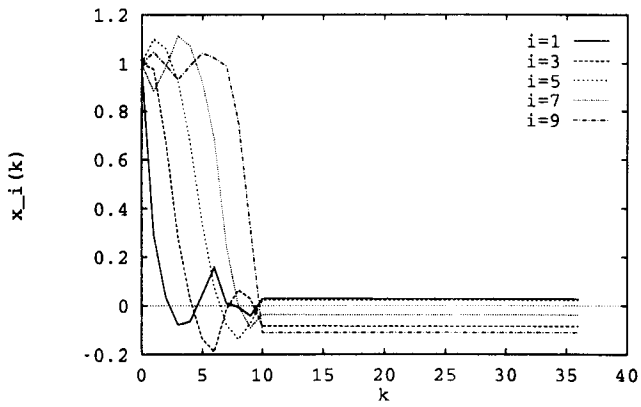


**Figure 21. Disturbance rejection for step disturbance.**

Lanes 1, 3, 5, 7, 9 vs. time.

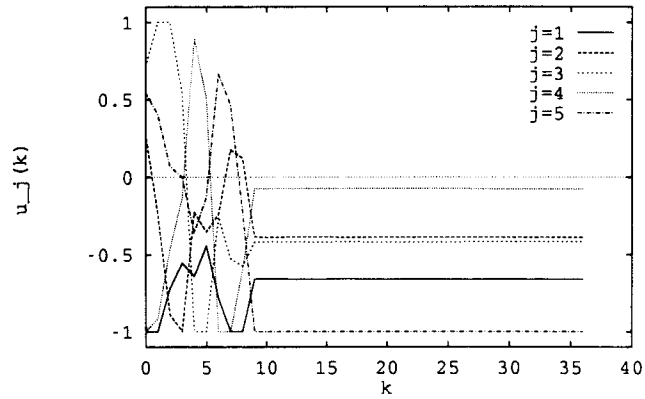


**Figure 22. Disturbance rejection for step disturbance.**

Actuators 1–5 vs. time.

does little to the remaining lanes, because the estimator has not had enough sensor information to known there is a disturbance in the other lanes. At time $k = 2$, the sensor passes over lane 2 and the state estimate of lane 2 is reliably updated. The control action taken at time 2 tries to eliminate simultaneously the estimated disturbances in lanes 1 and 2. Similar activity is shown at times 3–10. At time 10, the sensor has completed one sweep across the film and has concluded correctly that there is a disturbance in each lane. The succeeding sensor measurements provide little new information and the regulator returns the film gage to the setpoint shortly after $k = 10$. Notice that the steady-state control action and film gage are in agreement with the steady-state analysis of the previous section, as displayed in Figures 15 and 16. Recall that the steady-state offset is a result of there being only 5 actuators to control 10 lanes.

Some comments regarding the dynamic performance are as follows. First of all, it is apparent that the dynamic response of the estimator and regulator can be very fast. In the example, the film gage is returned to setpoint after only one sweep across all lanes. The control action that is taken is nonintuitive and would not result from some simple decoupling scheme. The multivariable interactions are very pronounced since the $K$ matrix is ill-conditioned. Although one could argue that it would be desirable from a maintenance point of view to have some simple pairing between actuators and lane gage measurement, that approach does not seem well suited to this process due to the strong coupling.

Secondly, the actuator constraints are handled cleanly with this approach. Notice that all five actuators hit constraints during the transient even though only actuator 5 is constrained at steady state. It would be a very complex procedure to try to assign some override and antireset windup strategy to deal with these constraints. The constrained regulator approach provides an intuitive statement of how the constraints should be handled. The fact that the actual control action taken can be complex and nonintuitive should not prevent implementation or maintenance of the controller.

We next examine an example that contains significant sensor noise. We expect that in this situation the controller tuning parameters must be chosen to trade off two competing objectives: fast dynamic response vs. low sensitivity to noise. Figures 23 and 24 display the response of the previous regulator/estimator to the same step disturbance, but with noise

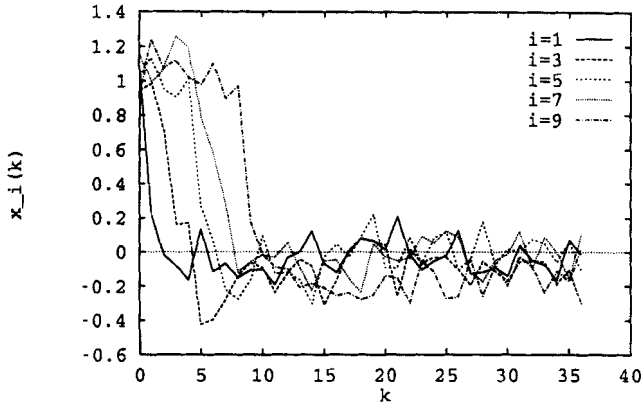


**Figure 23. Disturbance rejection for step disturbance with sensor noise.**

Lanes 1, 3, 5, 7, 9 vs. time.

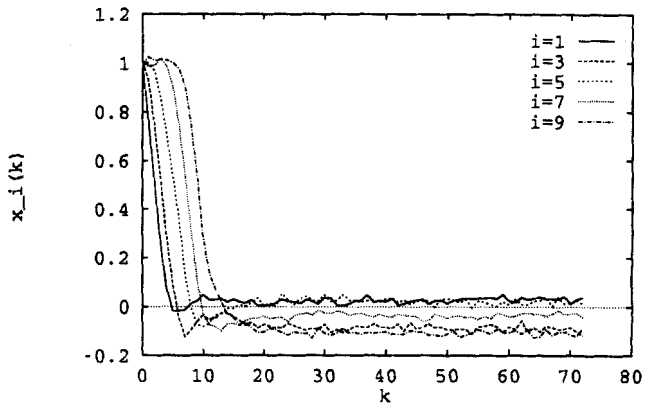


**Figure 25. Disturbance rejection for step disturbance with sensor noise and $S = 10$.**

Lanes 1, 3, 5, 7, 9 vs. time.

added to the sensor. Notice that the lanes are again all brought to zero quickly, but the manipulated variables are significantly more noisy. The erratic behavior in the inputs is exacerbated by the ill-conditioned $K$ matrix. For small changes in the estimated states (due to the sensor noise), large changes in the manipulated variable are computed by the regulator. The inputs can be made less erratic by clamping their time rate of change with constraints, penalizing their time rate of change by adding a penalty to the objective function, increasing the $\Gamma$ penalty in the regulator, or detuning the filter by increasing the noise covariance of the sensor noise, $R$. For illustrative purpose, we add a time rate of change penalty of the form

$$[u(k+1)-u(k)]^T S[u(k+1)-u(k)]$$

to the objective in Eq. QP4. Notice the effect of the penalty on the controller performance, shown in Figures 25 and 26 for $S = 10$. The inputs have become much smoother, the film gage has become only slightly more sluggish, and is also considerably less noisy. These two figures show that the previous tuning, based on the assumption of no noise in the sensor, gives the controller such high gain that it actually amplifies the sensor noise and adversely affects the film gage with excessive input manipulation. This is a prototypical example of overcontrolling the process. The controller should be tuned so that control action is an appropriate response to the reliability of the sensor information. The example illustrates that $S$ is one of the effective handles that can be used for this tuning. Setpoint tracking also has been investigated and results similar to those for disturbance rejection are obtainable.

## Conclusions and Recommendations

The research presented in this article is part of an ongoing effort to reduce the variability and improve the product quality in the manufacture of film and sheet products. We have described a linear modeling framework that is capable of describing many of the known features of these processes, including a noisy and moving gage sensor; significant process noise; strong coupling between the gages in different lanes; constraints on the actuators; and significant time delay between the actuators and the sensor. A model-predictive controller consisting of a constrained linear quadratic regulator and a time-varying Kalman filter is recommended for minimizing the gage variance and maximizing the product quality.

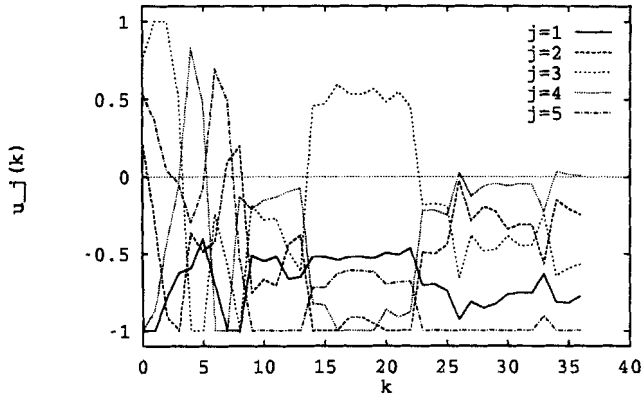


**Figure 24. Disturbance rejection for step disturbance with sensor noise.**

Actuators 1–5 vs. time.

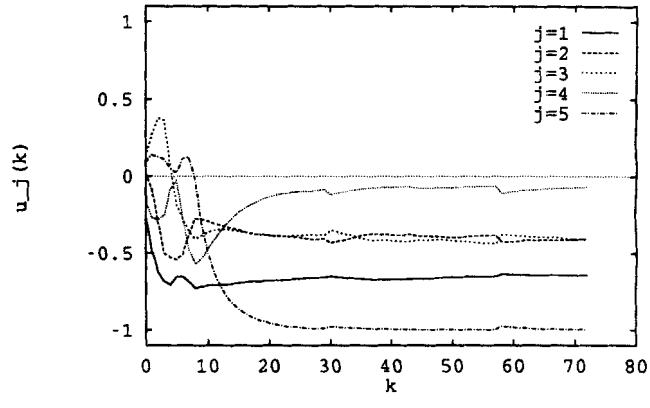


**Figure 26. Disturbance rejection for step disturbance with sensor noise and $S = 10$.**

Actuators 1–5 vs. time.

If the process exhibits more complex dynamics than are described in Eqs. 3 and 4, it is straightforward to extend the state vector to capture any dynamics of interest at the cost of increasing the model complexity.

The next step in the project is the identification of the process model and its associated uncertainty from plant data. The controller will then be tuned to account for the identified uncertainty and tested on a production line.

## Acknowledgments

The first author (J. B. R.) would like to thank the DuPont company and Drs. W. David Smith, Jr., and Babatunde A. Ogunnaike for making possible the five-month sabbatical during which this work was performed. Dr. Ronald K. Pearson is acknowledged for his many insightful discussions on filtering. Dr. Edwin J. Lightfoot provided many helpful comments on the original manuscript.

Dr. John W. Eaton of the University of Texas is gratefully acknowledged for developing the Octave software system with which all simulations were performed. Mr. Kenneth R. Muske of the University of Texas wrote the model predictive control routines with which the control calculations were performed.

## Notation

$d_l$ = lower bounds on change in inputs
$d_u$ = upper bounds on change in inputs
$D$ = input constraint matrix
$E$ = expectation of a stochastic variable
$G_x$ = correlation matrix for usual states in state-space model
$G_d$ = correlation matrix for augmented disturbance states
$I_n$ = identity matrix of order $n$
$m$ = number of actuators or inputs
$n$ = order of system
$v$ = stochastic output or measurement noise vector
$w$ = stochastic state noise vector
$\Phi$ = regulator objective function

## Literature Cited

Åström, K. J., *Introduction to Stochastic Control Theory*, Academic Press, San Diego, CA (1970).

Bergh, L. G., and J. F. MacGregor, "Spatial Control of Sheet and Film Forming Processes," *Can. J. Chem. Eng.*, **65**, 148 (1987).

Boyle, T. J., "Control of Cross-Direction Variations in Web Forming Machines," *Can. J. Chem. Eng.*, **55**, 457 (1977).

Braatz, R. D., M. L. Tyler, M. Morari, F. R. Pranckh, and L. Sartor, "Identification and Cross-Directional Control of Coating Processes," *AIChE J.*, **38**(9), 1329 (1992).

Bryson, A. E., and Y. Ho, *Applied Optimal Control*, Hemisphere Publishing, New York (1975).

Campbell, J. C., and J. B. Rawlings, "Estimation and Control of Film and Sheet Forming Processes," in *Proc. SIAM Symp. on Control Problems in Industry*, San Diego, CA (July, 1994).

Chen, S. C., "Kalman Filtering Applied to Sheet Measurement," *Proc. Amer. Control Conf.*, Atlanta, GA (1988).

Chen, S. C., and R. G. Wilhelm, Jr., "Optimal Control of Cross-machine Direction Web Profile with Constraints on the Control Effort," *Proc. Amer. Control Conf.*, Seattle, WA (1986).

Eaton, J. W., "Octave—A High-Level Interactive Language for Numerical Computations," Tech. Rep. CCSR-93-003, The Univ. of Texas Center for Control and Systems Research, Austin, TX 78712 (1993).

Francis, B. A., and W. M. Wonham, "The Internal Model Principle of Control Theory," *Automatica*, **12**, 457 (1976).

Lee, J. H., M. Morari, and C. E. García, "State-space Interpretation of Model Predictive Control," *Automatica*, **30**(4), 707 (1994).

Muske, K. R., "Linear Model Predictive Control of Chemical Processes," PhD Thesis, The University of Texas at Austin (1995).

Muske, K. R., and J. B. Rawlings, "Model Predictive Control with Linear Models," *AIChE J.*, **39**(2), 262 (1993).

Rawlings, J. B., and I.-L. Chien, "Gage Control of Sheet and Film Forming Processes," DuPont Accession Rep. 17944, E. I. du Pont de Nemours, Wilmington, DE (Aug. 27, 1993).

Rawlings, J. B., and K. R. Muske, "Stability of Constrained Receding Horizon Control," *IEEE Trans. Automat. Contr.*, **AC-38**(10), 1512 (1993).

Scokaert, P. O., and J. B. Rawlings, "Stability of Model Predictive Control Under Perturbations," *Proc. IFAC Symp. on Nonlinear Control System Design*, Tahoe City, CA (1995).

Tyler, M. L., and M. Morari, "Estimation of Cross Directional Properties: Scanning vs. Stationary Sensors," *AIChE J.*, **41**, 846 (1995).

Wilhelm, R. G., Jr., and M. Fjeld, "Control Algorithms for Cross Directional Control: the State of the Art," *Proc. IFAC/IMEKO Conf. on Instrumentation in the Paper, Rubber, Plastic and Polymerization Industries*, Antwerp (1983).

*Manuscript received Nov. 28, 1994, and revision received Apr. 10, 1995.*